

Gravitational Interactions in Poor Galaxy Groups

David S. Davis¹ and William C. Keel²

*Department of Physics and Astronomy, The University of Alabama, 206 Gallalee Hall,
Tuscaloosa AL 35487*

John S. Mulchaey

*The Observatories of the Carnegie Institution of Washington, 813 Santa Barbara St., Pasadena
CA 91101-1292*

and

Patricia A. Henning

*Department of Physics and Astronomy, The University of New Mexico, 800 Yale Blvd., NE,
Albuquerque, NM 87131*

ABSTRACT

We report the results of the spatial analysis of deep *ROSAT* HRI observations, optical imaging and spectroscopy, and high-resolution VLA H I and continuum imaging of NGC 1961 and NGC 2276. These spirals were selected as showing some previous evidence for interaction with a surrounding (hot) diffuse medium.

Our results favor most aspects of these galaxies as being shaped by gravitational interactions with companions, rather than the asymmetric pressure from motion through an external medium. The old stars follow the asymmetric structures of young stars and ionized gas, which suggests a tidal origin for the lopsided appearance of these galaxies. In NGC 2276, the H I and star-forming regions are strongly concentrated along

¹Present address: MIT Center for Space Research, Building 37-662B, Cambridge, MA 02139-4307

²Visiting astronomer, Kitt Peak National Observatory, National Optical Astronomy Observatories, operated by AURA, Inc., under cooperative agreement with the National Science Foundation.

the western edge of the disk. In this case, the ROSAT HRI detects the brightest star-forming regions as well as the diffuse disk emission, the most distant galaxy with such a detection. An asymmetric ionization gradient in the H II regions suggests radial movement of gas, which might have occurred in either tidal or wind scenarios. The X-ray emission from NGC 1961 is dominated by a point source near the nucleus of the galaxy but extended emission is seen out to a radius of $\sim 0'8$.

Previous studies of the enrichment of the intragroup medium in the NGC 2300 group indicates that stripping may be important in this system, but the density of the IGM is much too tenuous to effectively strip the gas from the galaxy. However, we propose that gravitational interactions in the group environment may enhance stripping. During a gravitational encounter the disk of the spiral galaxy may be warped, making ram pressure stripping more efficient than in a quiescent disk.

Subject headings: interstellar medium - X-rays: galaxies - galaxies: individual NGC 1961 - galaxies: individual NGC 2276

1. Introduction

The discovery of hot gas in clusters of galaxies presented the possibility that interactions between a galaxy and its environment could influence its evolution. A galaxy's motion through the cluster gas may play a role in the segregation of elliptical and S0 galaxies from gas rich spirals by stripping of the interstellar medium. Evidence that stripping does occur in clusters is strongest in the case of Virgo, where the spiral galaxies near the cluster center show a pronounced HI deficit associated with truncation and asymmetry of the H I disks (Cayatte et al. 1990) which is attributed to the hot cluster medium stripping HI gas from the galaxies. An extreme case may be found in NGC 5291 on the outskirts of the IC 4329 cluster, where a large H I mass is found outside the optical galaxy and systematically offset outwards from the cluster core, with intense star formation seen along the "upstream" sides of H I clumps (Longmore et al. 1979, Malphrus et al. 1995). There is evidence that this process also occurs for the hot gas seen in elliptical galaxies. The X-ray plume from M86 is thought to be due to stripping as the elliptical plunges into the hot cluster gas (Forman Jones & Tucker 1985; Irwin & Sarizan 1996). The discovery of diffuse gas in poor groups (e.g. Mulchaey et al. 1993; Ponman & Bertram 1993) raised the possibility that gas stripping could also occur in environments much less dense than that of clusters. Since the group environment is less dense than the cluster environment and the velocity dispersions of groups are also less, the effects of stripping should be more subtle than those seen in clusters. Nonetheless, optical and radio work has suggested that some spirals in rather sparse environments show evidence of interaction with a surrounding dif-

fuse medium. Confirmation of this process would be important in suggesting a new arena for environmental influences outside of rich clusters.

We report here new multi-wavelength observations of two of the strongest candidates for such interactions, NGC 1961 (Arp 184) and NGC 2276 (Arp 25 and 114), analyzed with the aim of distinguishing the gravitational effects of surrounding galaxies from hydrodynamic effects of surrounding gas. We trace the young and old stellar components as well as ionized, neutral, and X-ray gas, to distinguish the response to tidal perturbations, which is to first order similar for stars and gas, from the effects of a gaseous disturbance, inconsequential for old stars but manifest in low-density gas tracers.

These galaxies were selected as showing the most likely signatures of sweeping by a hot external medium based on radio and optical evidence. Radio studies of bright spiral galaxies (Condon 1983; Condon et al. 1990) identified a population of spiral galaxies with extraordinarily strong disk emission at centimeter wavelengths. Optical work shows that this is invariably linked to strong disk star formation, and often to interactions. The link to galaxy interactions is hardly unusual given the abundant evidence that tidal forces can induce star formation, but some of the most striking examples have no plausible nearby companion. In two of the best studied spirals of this kind (NGC 1961 and NGC 2276), there is no obviously interacting nearby companion and yet a strong asymmetry appears in the optical and radio maps, suggesting that these galaxies may be interacting with the intragroup medium rather than another galaxy. However, the galaxy environments of such groups have made the interpretation am-

biguous in each case; there is usually a bright galaxy close enough in projection to potentially act as a tidal perturber, perhaps several crossing times ago so that the interaction is not immediately apparent.

NGC 1961 is also notable for its exceptionally large linear size among spirals (Rubin, Roberts & Ford 1979 ; Romanishin 1983). Rubin et al. find that the optical rotation curve implies an encircled mass above $10^{12} M_{\odot}$, and mention a significant role for non-circular motions. This large mass is confirmed by Shostak et al. (1982) who map the galaxy using 21 cm spectral imaging. The rotation curve derived from the channel maps is well organized and implies a mass of $\sim 1.5 \times 10^{12} M_{\odot}$. The integrated H I map shows that the bulk of the neutral hydrogen emission is coincident with the optical galaxy, but the H I is also extended to the NW. This extension contains $\approx 10\%$ of the total H I mass. Faint spiral arms are seen in the optical image coincident with the H I extension. Opposite the H I extension, on the SW side of the galaxy, the H I distribution is sharply truncated. This H I morphology leads Shostak et al. (1982) to interpret this as stripping of the H I by the hot intergalactic medium. They noted rough coincidence of diffuse X-ray structure in an *Einstein* IPC image with an extended H I feature, and interpreted this as evidence of the hot stripping medium. However, ROSAT PSPC observations do not confirm the presence of such a hot cloud (Mulchaey et al. 1996).

NGC 2276 is a very luminous Sc I spiral, in the NGC 2300 poor group. This is the most H α -luminous galaxy in the Kennicutt and Kent (1983) survey, and is remarkable not only for its disturbed morphology but for a star formation rate high enough to have generated 4 observed supernovae within the

last 40 years, three of which were in the apparent “leading edge” and close to but not necessarily directly associated with bright H II regions (Iskudarian & Shakhbazian 1967, Shakhbazian 1968, Iskudarian 1968, Treffers 1993). While the elliptical NGC 2300 and the spiral NGC 2276 form a relatively isolated pair according to position-driven algorithms, they are rather far apart (≈ 150 kpc for $H_0 = 50 \text{ km s}^{-1} \text{ Mpc}^{-1}$), which at first glance makes a tidal origin for the asymmetric disk unlikely. The galaxy gained heightened interest with the discovery of a diffuse X-ray medium in its surroundings, the NGC 2300 group (Mulchaey et al. 1993).

The theme of our analysis is to ask whether we can distinguish the effects of gravitational interactions involving neighboring galaxies from those of ram pressure driven by a surrounding diffuse medium, and if so whether there is any strong evidence that ram pressure is responsible for the peculiar features of these galaxies. Both galaxies are members of poor groups (Maia, da Costa & Latham 1986) so that their distorted morphologies might be interpreted as evidence for a recent interaction with another galaxy in each group.

2. Observations

2.1. ROSAT X-ray Observations

NGC 1961 and NGC 2276 were observed by the *ROSAT* PSPC and the HRI. The combination of these two instruments allows the spectral and spatial properties of the X-ray emission for the galaxies in this group to be determined. The useful HRI exposure for NGC 1961 is almost 83 ksec and that for NGC 2276 is about 74 ksec. A log of observations is given in Table 1.

The *ROSAT* PSPC observed NGC 1961

for 14.8 ksec in March of 1993. The galaxy was 10'4 off-axis. The total exposure time for NGC 2276 is \sim 23ks and is divided between three different exposures. While the galaxy is within the central 20' ring of the PSPC, no useful spatial information was derived from these observations. However, the PSPC observations of NGC 1961 and NGC 2276 allow us to fit a spectral model to the X-ray emission from these galaxies and thus accurately determine the X-ray flux from these galaxies.

2.1.1. PSPC Spectral Results

To determine the flux from an object detected with the *ROSAT* HRI some information about the spectral characteristics of the object must be known. The HRI provides only very crude (\sim two channel) spectral information. However, with the addition of PSPC data a spectral model can be determined which can then be used to derive an accurate conversion from HRI counts to flux.

The spectra for NGC 1961 and NGC 2276 were extracted from each field with the background determined locally. The galaxy spectrum was extracted using a 3' circle centered on the galaxy position. The background was taken from an annulus with an inner radius of 3' and an outer radius of 6'. NGC 1961 has a total of 215 net counts (0.146 counts s^{-1} 0.5 - 2.0 keV) in a 3' circle centered on the galaxy. The spectrum is rebinned so that each channel has a minimum of 25 counts and the poorly calibrated channels (Snowden 1994) are dropped from the spectral fit. This results in a spectrum with 8 channels. We fit the resulting spectrum with a Raymond-Smith plasma model with the Galactic absorption fixed at 9.13×10^{20} atoms cm^{-2} (Starke et al. 1992). The best fit temperature is $0.67^{+0.19}_{-0.24}$ keV, where the errors are the 90% confidence

levels for a single interesting parameter. The abundance is constrained to be <3.4 solar at the 90% confidence level. The best fit has $\chi^2 = 2.38$ for 5 degrees of freedom. The flux from this galaxy is 1.79×10^{-13} erg s^{-1} cm^{-2} . At the assumed distance for this galaxy (79.7 Mpc) the soft X-ray luminosity is 1.36×10^{41} erg s^{-1} .

NGC 2276 is in three PSPC fields and at a different position in the PSPC in each exposure. We extracted the spectrum from each of the fields as described above and fit the resulting spectra simultaneously with XSPEC. For the initial observation of NGC 2276 (rp900161) rebinning the spectrum results in 5 useful channels. For the two remaining observations this rebinning results in 9 channels between 0.4 and 2.0 keV with sufficient counts to justify spectral analysis. The three fields yield a total of 371 counts for NGC 2276 which corresponds to a count rate of 0.021 counts s^{-1} . We attempted to fit a Raymond-Smith plasma with Galactic absorption to the spectrum but the fit yields unphysical temperatures, $kT > 5$ keV and $N_h \sim 0$. Since the Raymond-Smith model gave unacceptable results we fit a simple power law model with Galactic absorption to the data. The photon index of the best fit power law ($\chi^2_\nu = 0.47$ for 17 dof) is -1.42. The X-ray flux in the 0.4 - 2.0 keV band is 7.26×10^{-12} erg cm^{-2} s^{-1} , which for the assumed distance to this group of 45.7 Mpc ($H_0 = 50$ km s^{-1} Mpc^{-1}) yields a luminosity of 1.82×10^{42} erg s^{-1} . The Galactic column has been fixed at 3.2×10^{20} cm^{-2} , the value given by Stark et al. (1992).

2.1.2. HRI Spatial Results

To determine any X-ray structure in these two galaxies the *ROSAT* HRI data must be corrected for known spatial irregularities.

This is accomplished by flat fielding the images using the procedures outlined in Snowden et al. (1994). The exposure maps are generated using information of the aspect and wobble of the satellite along with a map of the known detector irregularities. Using this information a map can be generated which accurately reproduces the spatial variations for each observation. The data and resulting exposure maps are binned in $5''$ pixels. The data are then divided by the exposure map to generate the flat fielded image, which is used in the spatial analysis below.

2.2. NGC 1961

The flat-fielded HRI data, with $5''$ pixels and smoothed with a Gaussian ($\sigma=10''$), for NGC 1961 are shown overlaying a digitized Sky Survey (blue-light) image in figure 1. The centroid of the X-ray emission is at $5^h 42^m 04^s.3 +69^\circ 22' 46''$, in excellent agreement with the optical position of the galaxy given in the RC3. The counts for this source are extracted using a circle with a radius of $6.5'$ centered at the peak of the X-ray emission. The net number of HRI counts in the galaxy is 447.7 ± 60.43 counts, which corresponds to a count rate of $5.46 \times 10^{-3} \pm 0.74 \times 10^{-3}$ counts s^{-1} . Analysis of the X-ray profile of NGC 1961 shows that the X-ray emission is extended. Figure 2 shows the profile of NGC 1961 and the profile of a point source in the same field. The point source is only $\sim 2.5'$ from the position of NGC 1961 and has been scaled to match the counts in the inner $0.2'$. An excess of counts can be seen between $0.25'$ and $0.8'$ from the center, and is 272 counts (3.32×10^{-3} counts s^{-1}). Using the flux determined from the PSPC observation of this galaxy we determine the conversion factor between counts s^{-1} and flux to be

0.305×10^{11} counts cm^2 erg^{-1} . Assuming that this also holds true for the diffuse component alone, we obtain a flux of 1.09×10^{-13} $erg s^{-1} cm^{-2}$ which at the assumed distance of the galaxy corresponds to an X-ray luminosity of 8.31×10^{40} $erg s^{-1}$.

2.3. NGC 2276

The HRI data for NGC 2276 have been resampled into $5''$ bins and then smoothed with a Gaussian with $\sigma=10''$. Figure 3 shows the B band image of NGC 2276 with the X-ray contours from the smoothed image overlaying the optical image. Two prominent regions of X-ray emission can be seen; the strongest is to the northwest of the nucleus and is a 12σ peak. The nucleus of the galaxy is also an X-ray source and is at $7^h 27^m 21^s +85^\circ 45' 13.9''$. X-ray emission from the disk of the galaxy can be seen around the nuclear region and along the western edge of the disk.

The total counts from the galaxy were determined using a circle with radius $90''$ centered on the nuclear X-ray emission from the galaxy. The background is determined using an annular ring with an inner radius of $90''$ and an outer radius of $180''$ from the center of the galaxy and all point sources were removed from this annulus. The background subtracted HRI count rate for this galaxy is $1.33 \times 10^{-2} \pm 0.12 \times 10^{-2}$ counts s^{-1} . Using the spectral fit from above we can then derive the conversion between HRI counts and flux as 0.203×10^{11} counts cm^2 erg^{-1} . Using an elliptical aperture ($22'' \times 37''$) centered on the peak of the emission from the northwest quadrant of the galaxy, we determine the count rate is $5.58 \times 10^{-3} \pm 0.73 \times 10^{-3}$ counts s^{-1} , which corresponds to an X-ray luminosity of 7.26×10^{41} $erg s^{-1}$. The count rate from the nuclear region is $2.58 \times 10^{-3} \pm 0.32 \times 10^{-3}$

counts s^{-1} which corresponds to an X-ray luminosity of $3.2 \times 10^{41} \text{ erg s}^{-1}$ in a $22''$ circular aperture. This implies that the X-ray luminosity from the disk of this galaxy is at least $7.9 \times 10^{41} \text{ erg s}^{-1}$.

3. Optical Data

Images in a variety of passbands and spectral data were acquired for both galaxies to trace both young and old stellar components. Narrow-band images, with filters (of typical bandwidth 60 \AA) isolating $\text{H}\beta$, $[\text{O III}] \lambda 5007$, $\text{H}\alpha + [\text{N II}] \lambda 6583$, and $[\text{S II}] \lambda\lambda 6717 + 6731$ at each galaxy's redshift, along with adjacent continuum bands at 5125 and 6694 \AA for continuum subtraction, were obtained at the KPNO 2.1m telescope with the video-camera system in October 1983. The field of view was 140 arcseconds, well matched to the size of NGC 2276 and requiring two pointings for NGC 1961 (so that only the central part was observed in the $\text{H}\beta$, $[\text{O III}]$, and $[\text{S II}]$ passbands). Additional broad-band images were obtained with CCDs for NGC 2276 (in B at the KPNO 2.1m and BVRI at the Lowell 1.1m) and NGC 1961 (BRI and narrowband for $\text{H}\alpha$). The Video Camera data used a combination of internal quartz and night-sky flat fields, with geometric distortions produced by the image-tube chain corrected after flat-field division. Since this corrects to constant surface-brightness (rather than point-source) response, the H II region fluxes required a modest correction (reaching 25% only at the extreme corners) to recover accurate integrated fluxes. The correction (which amounts to the Jacobean of the local coordinate transformation) was derived from observations of photometric standard stars in NGC 2419. The device was quite stable for these observations, with none of the Moire

patterns which sometimes plagued such data. Thus, the fluxes should be reliable at the 15% level for all but the faintest H II regions; issues of blending and size definition are more important error sources than known instrumental effects.

3.1. NGC 1961

The optical morphology of NGC 1961 is somewhat confused by inclination issues. The outer regions alone would indicate a substantially inclined spiral pattern, seen perhaps 45° from the plane. However, the inner isophotes are almost circular in regions devoid of obvious extinction; the usually flattened bulge geometry of spirals would suggest that this area is seen nearly face-on. The dust lanes cut this bulge strongly, obviously at a significant angle to the sky plane. One might view the system as being strongly warped, with the bulge and inner spiral features north of the nucleus seen close to the plane of the sky and the outer arms plus inner dust features seen about 40° from edge-on. The very disturbed nature of the disk makes normal morphological classification (as well as inclination estimates) more guesswork than we might like. The apparent pitch angles of the arms to the north and east are inconsistent with the dust geometry just south of the nucleus, and the more open arms to the west, for any simple coplanar geometry.

The disk must be far from the plane of the sky in order to give the very large rotation velocities measured by Rubin et al. (1979), where the *observed* velocities before any inclination correction are among the largest ever seen in a spiral disk. However, beyond this, analysis of the geometry is limited; in the words of Rubin et al., "It is difficult to know just how much symmetry we can force on NGC 1961".

For NGC 1961, aperture spectra of the nucleus and several of the brightest complexes of H II regions were obtained using the KPNO 2.1m and Intensified Image-Dissector Scanner (IIDS) with 6.1" circular apertures and the Mount Lemmon 1.5m telescope and similar scanner (4.7" apertures), in late 1983. The line properties from the aperture spectrophotometry of both galaxies are listed in Table 2. Numerous additional regions could be measured in at least H α after calibrating the narrow-band images via the aperture measurements (typically with 5-arcsecond apertures). Properties of these additional regions for both NGC 1961 and NGC 2276 are given in Table 3. The intent was to select the ones bright enough for meaningful line ratios, rather than a sample complete in H α flux. The table includes as well equivalent widths of H α emission, measured in the same 5" apertures, as a guide to the emission-line contrast of each association.

A more complete listing of H II regions in NGC 1961 is provided; these are relatively better separated and physically larger (typical H α FWHM 4" \approx 1 kpc) than we see in NGC 2276, so at the distance of NGC 1961 it is more appropriate to speak of H II complexes rather than individual H II regions.

3.2. NGC 2276

The line images for NGC 2276 were calibrated by means of aperture spectrophotometry of the brightest two H II regions, obtained using 8" apertures with the Intensified Reticon Scanner (IRS) at what was at the time (January 1984) the #1 0.9m telescope at KPNO. Use of such a small telescope was driven by the inability to use the 2.1m with IIDS spectrograph within 5° of the celestial pole. The H II regions were acquired

by blind offsets from the 8th-magnitude star SAO 001148 (only 2.4 arcminutes from NGC 2276), since even the galaxy nucleus could not be seen through the guiding eyepiece. Using these data to set the absolute intensity scales for the line images, and assuming that the [N II]/H α ratios in these areas are typical, allows measurement of the intensities of all four lines for any desired location from the images. A lower-resolution slit spectrum, obtained with the KPNO 4-meter telescope and Cryogenic Camera, was obtained with an east-west slit position crossing the nucleus, to get spatially continuous coverage of the [O III]/H β ratio and measure the [N II]/H α ratio with higher confidence.

The broad-band images are useful in distinguishing the young stellar population (H α and blue light) from the older population which should be unaffected by purely gas-dynamical processes (dominating the I-band light). In NGC 2276, all show the same characteristic truncation at the western edge (Figure 3), which in itself suggests that gravitational effects produce the asymmetry (as discussed by Gruendl et al. 1993). The eastern part of the disk, with a much lower mean star-formation rate as measured from H α , appears normal, with a smooth intensity profile and no such truncation.

Figure 4 shows the distribution of H α emission. H α imaging traces the distribution of OB stars and hence recent star formation. Figure 4 shows that the H α flux from this galaxy is very asymmetric, with the majority of H α flux originating from the western side of the galaxy. The truncated side of the galaxy disk is lined by HII regions while the eastern half of the galaxy has only a handful of H α knots. The H α flux from the nuclear region is 1.96×10^{-13} erg s $^{-1}$ cm $^{-2}$. The integrated

$\text{H}\alpha$ flux from the galaxy is 3.39×10^{-12} erg s $^{-1}$ cm $^{-2}$.

Line-ratio measurements show another aspect of this asymmetry - not only is the distribution of H II regions different on the two sides of the galaxy, so is their ionization. While both sides of the galaxy show the familiar abundance-linked gradient in [O III]/H β , this gradient is twice as steep on the western (“upstream”) side of the disk. Such a situation might be found if, for example, disk gas on this side had been swept inward from its original position by whatever process. A similar azimuthal structure to the ionization gradient has been reported for M101 (Kennicutt & Garnett 1996), at a lower level. It may be relevant that the optical disk of M101 is also rather asymmetric, at a level difficult to reconcile with the faintness of its immediate companion NGC 5474. We are not aware of any detailed modelling of the chemical results of gas sweeping within a disk, so only schematic considerations can be applied. The diffuse gas (represented observationally by H I) will be driven inward on the “upstream” side, perhaps with material dropping out of the radial flow as some gas condenses to a much denser molecular form with correspondingly smaller cross-section for pressure-driven acceleration. To first order, the abundance gradient will be the ratio of initial and final galactocentric distances, whether this distance is the total radial flow or the motion to dropout from radial flow. Such an externally-driven change in the abundance gradient will persist for an orbital time or so, since clouds initially at similar radii may have different radial velocities and thus radial diffusion driven by their different orbits will set in. This may be seen from typical n -body models for perturbed disks, for example shown well in

the high-inclination models by Howard et al. (1993).

The optical data for NGC 2276 has been re-sampled and smoothed so that the resolution matches that of the X-ray data and then fluxes were extracted from regions which match the X-ray regions. Table 4 lists the flux and luminosity determined for the different regions discussed in §4.2. These values allow us to compare the stellar populations as revealed through their X-ray sources as well as the direct starlight and recombination radiation.

4. Radio Data

VLA³ synthesis maps at 1.4 and 5 GHz were obtained using data from the A & B array. These data were combined and cleaned using APCLN to obtain the final images. The final resolution is $\sim 4''$. Both these galaxies exhibit strong and small radio sources associated with luminous H II regions, as noted by Condon (1983).

4.1. NGC 1961

The radio morphology of NGC 1961 at 20cm (figure 5) is quite similar to that seen in the B-band image. Diffuse emission can be seen around the nucleus and a ridge of emission can be seen about 1' to the south which corresponds to a spiral arm seen in the optical image. The 20cm flux from NGC 1961 within 60'' is 150.6 mJy. The strongest individual source in this galaxy is the nucleus at 10.61 mJy. Several pointlike sources can be seen to the west of the nuclear region and

³The National Radio Astronomy Observatory is a facility of the National Science Foundation operated under cooperative agreement by Associated Universities, Inc.

these are labeled in figure 5. Knot 1 has a flux of 4.26 mJy; knot 2's flux is 2.61 mJy; knot 3 has a flux of 0.94 mJy. Subtracting the flux from these sources from the total flux from the galaxy yields a flux of 132.2 mJy for the diffuse component.

4.2. NGC 2276

The 20cm radio data shown in figure 6 reflects the morphology of the optical data discussed above. The southwest edge of NGC 2276 appears to end abruptly and there are at least five radio bright sources within 15" of the truncated edge of the radio disk. To the east no sharp boundary is seen and the radio emission gradually is lost in the noise. The extent of the diffuse radio emission on the eastern side of the galaxy is approximately twice that of the truncated side. However from figure 6 it is clear that the majority of the diffuse radio emission from this galaxy is from the truncated side of the galaxy. The total radio emission from this galaxy is 282.5 mJy. The nuclear region is comma shaped with the tail of the comma appearing to lead into a spiral arm. One strong point source can be seen to the northwest of the nucleus along the edge of the radio emission. The nuclear region is the strongest point-like source and using a 6" aperture we find that the emission from the nucleus is 14.41 mJy. The point source on the northwest edge of the radio emission has a flux of 6.27 mJy. Subtracting the point source emission from the total gives a flux in the diffuse component of 261.8 mJy.

The morphological relation between H α and radio continuum emission can be quantified through a "smearing relation". Pieces of the H α image were convolved with various assumed streaming lengths, locally along the arm pitch. The best match occurs for a typi-

cal value of 8" (2 kpc). That is, if the particles giving rise to the synchrotron emission at centimeter wavelengths are mostly injected by supernovae close to the locations of present H II regions, they travel typical distances along the large-scale magnetic fields of 2 kpc.

Several luminous H II regions in both NGC 1961 and NGC 2276 contain strong nonthermal radio sources, compact on 1-arcsecond scales. The most prominent is the bright H II region 40" W and 19" N of the nucleus in NGC 2276, which is brighter than the nuclear source at 20 cm. The reason for this exceptional emission is unclear. Supernova remnants (SNR) in dense environments might be temporarily very bright, although we did not detect any enhanced [S II] emission from shocks in these regions. Quantitatively, SNR show line ratios [S II] $\lambda\lambda 6717, 6731/\text{H}\alpha$ of 0.4 and larger (D'Odorico 1978, Dopita et al. 1984). This criterion has proven effective in identifying SNR in galaxies of the Local Group (Long et al. 1990), although at larger distances blending with neighboring H II regions and the diffuse ISM reduces the purity of the samples found in this way (Blair & Long 1997). By this criterion, a single emission region (number 10 in our listing) stands out both in [S II]/H α and [O III]/H β in the direction expected for shocked gas in a SNR. This is, however, not a detected 20-cm source; all the radio-bright regions have typical values of [S II]/H α in the range 0.18–0.28. If number 10 is a single SNR, it falls in the class of extraordinarily luminous remnants so far populated only by the remnant in NGC 4449 (Blair et al. 1983), with comparable emission-line luminosity but considerably lower ionization (since the NGC 4449 remnant was not detected in [S II] by Blair et al.). Any substantial population of SNR accounting for the

radio emission is either masked by the surrounding emission of normal H II regions or obscured by dust (at levels somewhat lower than the NGC 4449 SNR, so that our limits are mildly interesting but not as compelling as one might like).

The 21-cm HI line data, obtained with the VLA in C array, also reflect the asymmetric morphology seen in the other wavebands. The emission is sharply peaked along the western edge of the galaxy (Fig 7.) The integrated HI flux (16 Jy km/s) lies within the range of values reported for single-dish observations of NGC 2276 (Huchtmeier and Richter 1989).

5. Summary of Observations

The data for NGC 1961 show that the optical broad band and line emission from this galaxy are fairly symmetric in the inner regions. The X-ray and radio images are also fairly regular. The only exception to this is that in the radio image the southern spiral arm appears to have enhanced emission when compared with the northern spiral arm. The X-ray emission is peaked on the optical and radio nucleus of the galaxy and is mostly point-like, but an extended component can be seen. The extended X-rays appear to be elongated in the east-west direction, as is the optical image (see figure 1). At the lowest contour level, a weak tail-like feature can be seen extending to the southeast of the nuclear region, which might indicate that some of the hot ISM from the galaxy is being stripped. However, since this contour is only 3σ above the background it should be interpreted with caution, and it is the opposite direction of the neutral hydrogen tail seen by Shostak et al. (1982).

In contrast to NGC 1961, NGC 2276 appears highly asymmetric in all wavebands.

The western, or truncated, side has enhanced X-ray, optical, and radio emission when compared to the eastern half. The optical emission lines of [O III] and [S II] are restricted to the sharp boundary along the western limb of the galaxy. The diffuse X-ray emission can be seen along the truncated side of the galaxy in figure 3, along with the X-ray bright region to the northwest of the nuclear region. The X-ray contours give an impression of being swept back in the same direction as the optical and HI images.

6. Discussion

The goal of these observations is to determine if stripping of the ISM is occurring in these two groups. By using a combination of X-ray, optical, and radio imaging, along with spectroscopy, we find that the effects of the group is at least as complex as the analogous process in clusters (Moore et al. 1996). Ram pressure stripping or gravitational interactions alone are insufficient to explain the data. We find evidence that stripping of the ISM *and* gravitational interactions are affecting the galaxies.

6.1. NGC 1961

The HI distribution in NGC 1961 is strongly suggestive that stripping of the neutral gas is occurring (Shostak et al. 1982). However, the PSPC data for this group do not show the presence of hot intragroup gas and the upper limit for X-ray emission is $<1.5 \times 10^{41}$ erg s $^{-1}$ (Mulchaey et al. 1996). Thus, any gas which is present in the group to strip the HI must be too cool to be detected using the PSPC data or too diffuse to be separated from the X-ray background.

Tracers of star formation and supernova

remnants show that in the inner regions of NGC 1961 the star formation is symmetrically distributed about the nuclear region. Low resolution radio maps show that the HI (Shostak et al. 1982) and the 20cm emission is compressed along the northern edge and much flatter along the southern edge, again suggesting that stripping may be occurring in this galaxy. However, the high resolution 20cm map (fig 5) shows that this may be the result of the southern spiral arm being distorted and pulled further (at least in projection) from the nuclear region. The distorted spiral arms seen in the radio map (fig 5) are also evident in the B-band image. The stellar and the gaseous component are distorted in the same manner, which is not plausible with ram pressure stripping.

As has been found in the optical and far-infrared bands, there is reason to expect interactions to enhance the X-ray luminosity of galaxies. This would happen through enhancement of star formation, with the X-ray emission driven by massive stars and supernovae, and through producing a global hot (expanding) medium if the star-formation rate is high enough to produce an unbound, outflowing gas. Detailed studies of individual objects show that these processes can be seen, but there is yet no statistical study of the overall situation. Observations of the well-known interacting pair NGC 4038/9 with the *ROSAT* PSPC (Read et al. 1995) and *ASCA* (Sansom et al. 1996) show that emission is seen both from the giant H II regions and galaxy nuclei, and from a global, approximately bipolar gas interpreted as an outflow, as has been seen in some more powerful IR-bright or merging systems. At this point, it seems likely but unproven that interactions increase the X-ray luminosity of galaxies.

In this context, we note that the *Einstein* IPC X-ray luminosity (0.2 - 4.0 keV) of NGC 1961 is 2.40×10^{41} erg s⁻¹ which is not unusual for the blue luminosity of the galaxy (Fabbiano, Kim & Trinchieri 1992) and thus the X-ray luminosity does not seem strongly enhanced. The X-ray emission from NGC 1961 is mostly point-like in the HRI data and the peak emission is spatially coincident with the nucleus of the galaxy. This implies that most of the X-rays are from a region less than ~ 5.8 kpc across. Using the total luminosity of the galaxy and the luminosity of the extended component we determine the point source has a luminosity of 7.25×10^{40} erg s⁻¹.

Since interactions are also known to enhance star formation and Condon, Frayer & Broderick (1991) classify this galaxy as a starburst based on the ratio of infrared to radio flux, we compute the star formation rate. The star formation rate for this galaxy can be estimated from its far-infrared luminosity. The total far-infrared luminosity from 43 to 123 μ m is given by $L_{\text{IR}} \approx 6 \times 10^5 D^2 (2.58f_{60\mu\text{m}} + f_{100\mu\text{m}})$ (Lonsdale et al. 1985; Thronson & Telesco 1986) with D being the distance to the galaxy in Mpc. Using the measured IR $60\mu\text{m}$ flux of 6.60 mJy and the $100\mu\text{m}$ flux of 22.07 mJy, we find $L_{\text{IR}} = 1.49 \times 10^{11} M_{\odot}$. From this we find the SFR = $31 M_{\odot} \text{ yr}^{-1}$ for the high mass stars alone (Thronson & Telesco 1986), which translates to about $150 M_{\odot}/\text{yr}^{-1}$ for all stars assuming a Salpeter IMF. While NGC 1961 is a very luminous galaxy (listed as the most luminous galaxy of any type in the Revised Shapley-Ames Catalog, with $M_B = -23.7$), so that an extensive measure of SFR such as this would be unusually high even without a burst, such a high SFR requires a burst even for a galaxy this large and bright. To

get an intensive measure of recent SFR behavior, we derived an integrated $\text{H}\alpha + [\text{N II}]$ strength via integration in the narrow-band images, which yields an equivalent width of the sum of these lines of 35.5 \AA , and flux of $6.3 \times 10^{-12} \text{ erg cm}^{-2} \text{ s}$ in $\text{H}\alpha$ alone, using the spectroscopic value for $[\text{N II}]/\text{H}\alpha$, giving a luminosity of $L(\text{H}\alpha = 7 \times 10^{42} \text{ erg s}^{-1}$ including a somewhat uncertain correction for foreground extinction. While the $\text{H}\alpha$ luminosity corresponds to a large SFR ($62 \text{ M}_\odot/\text{yr}^{-1}$ using a Salpeter IMF), as implied by the total FIR strength, the equivalent width corresponds to a rather mild or very protracted burst (following, for example, Kennicutt et al. 1987). This may thus be a starburst galaxy, though the overall SFR would be high in any case since this is such a luminous (presumably massive) galaxy. The high SFR might be due to an interaction, especially since the morphology suggests disturbances in the outer spiral pattern. While the star formation is quite widespread, this cannot argue strongly either for or against an enhancement from interactions, since the distribution of H II regions in clearly interacting spirals span a wide range in radial and azimuthal distributions (Keel et al. 1993).

The similarity of the distortions seen in the gas and stars cannot be explained using ram-pressure stripping. The coincidence of the gaseous and stellar components argues that ram-pressure stripping plays little if any role in affecting the morphology of this galaxy in the inner regions. However, the HI distribution is indicative of stripping, thus it may be that both processes are occurring.

If a gravitational encounter has distorted the disk of the galaxy, then the gas distribution can become complex forming tails and ring structures (Moore et al. 1996). Even if

the stars and gas are initially bent out of the plane of the galaxy together, this can expose a larger area of the gas disk to the intragroup medium and this would make ram pressure stripping much more likely. Also HI disks are often substantially more extended than stellar disks, so if the group does contain gas, it would take much less gas to strip the HI gas in the outer disturbed portion of the disk than the gas farther in, where the starlight is easily detected. Thus, the group gas might remain diffuse enough to remain undetected in the *ROSAT* PSPC data and still generate the swept-back appearance of the HI data. So given the plethora of data on this galaxy it seems that the most likely scenario is that NGC 1961 has undergone a gravitational encounter, which has distorted the stellar and gaseous components of the disk, disturbed the spiral arms, slightly enhanced the star formation rate, and allowed ram-pressure stripping to remove the outer part of the original HI disk.

6.2. NGC 2276

This spiral galaxy was initially selected for study because of its unusual optical morphology. The optical continuum and emission line morphology of this galaxy is very asymmetric, with the bulk of the line emission from the western side of the galaxy. This is also reflected in the radio maps of this galaxy where the brightest 20cm emission is confined to the western half of the galaxy.

The X-ray morphology of NGC 2276 follows the optical and radio morphology of the galaxy. In contrast to NGC 1961, the nuclear source in NGC 2276 is not the strongest source; the disk emission along the western edge of this galaxy is just over twice the luminosity of the nuclear region. The total

$\log(L_x/L_{opt})$ is -1.82 while the average L_x/L_{opt} for late type spirals ($T=4-10$) is -6.90 ± 0.27 (Fabbiano, Gioia & Trinchieri 1988). The $\log(L_x/L_{FIR})$ is -2.36 , close to -3 as expected for normal galaxies or LINERS (Green, Anderson & Ward 1992) but not typical of starburst galaxies which have $\log(L_x/L_{FIR}) \approx -4$ (Heckman, Armus & Miley 1990).

The star formation rate can be estimated from the $H\alpha$ luminosity, which for NGC 2276 is 3.39×10^{41} erg s $^{-1}$. Using $SFR = 7.07 \times 10^{-42} \eta^{-1} L_{H\alpha} M_{\odot}$ yr $^{-1}$ (Hunter et al. 1986) and $\eta=0.5$, we estimate a star formation rate of $\sim 5 M_{\odot}$ yr $^{-1}$. Using the measured IR $60_{\mu\text{m}}$ flux of 11.97 mJy and the $100_{\mu\text{m}}$ flux of 28.96 mJy, we find that the $SFR = 15 M_{\odot}$ yr $^{-1}$. This is in reasonable agreement with the SFR derived from the $H\alpha$ flux given that these estimates are likely to be accurate only to within a factor of two. As in the case of NGC 1961, it is useful to consider an intensive quantity such as $H\alpha$ equivalent width to assess the history of the SFR. The integrated spectral data presented by Kennicutt (1992) give an $H\alpha$ equivalent width of 59 \AA , to be compared with the 32 \AA from aperture photometry by Kennicutt et al. (1987). This falls well above the range populated by smoothly declining SFR models (as shown in Kennicutt et al. 1987), putting this in the global-burst category.

The unusual morphology of this galaxy has been attributed to either ram pressure stripping or from a gravitational interaction with NGC 2300, an elliptical with signs of a recent merger (Forbes & Thomson 1992, who find evidence that it hosts a cooling flow). We have examined this object further, via analysis of a Lowell I -band image, to confirm the reported shell-like morphology. By subtracting the best overall $r^{1/4}$ model, we confirm the tidal extension and western “shell” reported

by Forbes & Thomson, and detect as well a nearly symmetric “bowtie” structure within about $15''$ of the nucleus (the edges of which appear in their residual image as 4θ residuals). All of these features are evidence for various levels of gravitational interaction.

Davis et al. (1996) and Mulchaey et al. (1993) show that the density of the intragroup medium itself is too small to significantly perturb the ISM of the galaxy. Gruendl et al. (1993), using Fabry-Perot observations of the $H\alpha$ velocity field, conclude that a tidal interaction with NGC 2300 is the most likely explanation for the truncated stellar disk and $H\alpha$ velocity field. Given the large projected separation between the galaxies, about 150 kpc, if the transverse relative velocity is in the range expected from velocity dispersions in small groups < 400 km s $^{-1}$, the encounter would have been nearly parabolic and taken place more than 4×10^8 years ago. This is a long time for immediate interaction effects to play out, suggesting that perhaps internal disk modes excited by the interaction continue to enhance the star formation even well after the perturber has departed.

From these lines of evidence, it appears that the morphology of NGC 2276 is primarily being affected by a gravitational encounter which has disturbed the stellar and gaseous component, enhanced the star formation rate along the truncated side of the galaxy, and again pulled the HI out of the plane of the galaxy so that stripping is much more likely. The vigorous star formation along the truncated side of the galaxy may be enhanced by ram pressure but it cannot be the dominate force shaping the morphology. The interaction might be important in making some of the disk H I much more vulnerable to stripping than it would have been originally, so

that the combination of two effects is not complete coincidence.

7. Conclusions

We have used the *ROSAT* HRI to study the X-ray emission from the disk of two spiral galaxies in small groups, NGC 1961 and NGC 2276. To the best of our knowledge these are the most distant spiral galaxies to have their X-ray disk emission resolved. The X-ray structure of NGC 1961 consists of a nuclear point-like source and diffuse emission from the disk. The nuclear source has an X-ray luminosity consistent with that of a low level AGN. The X-ray luminosity of the disk is 8.31×10^{40} erg s $^{-1}$ and is consistent with that seen from other normal spiral galaxies.

The disk emission from NGC 2276 is clumpy and is strongly correlated with the bright star forming regions seen on the western side of the galaxy. The X-ray luminosity of the disk component is 7.9×10^{41} erg s $^{-1}$, again not unusual for spiral galaxies of this blue magnitude. The nuclear region is also detected with a luminosity of 3.2×10^{41} erg s $^{-1}$ indicating that this galaxy may also have an active nucleus.

Tidal interactions have been shown to enhance the star formation in galaxies on both nuclear and global scales (Keel et al. 1985, Bushouse 1987, Kennicutt et al. 1987; also see references in Keel 1991) to an extent which is consistent with the H α luminosity and star formation rates derived above. So from the evidence we have presented above it appears that the strong star formation and distorted morphologies of these two spiral galaxies is most likely due to a tidal interaction with a companion galaxy and not due to ram pressure effects. However, the swept back appearance of the HI gas indicates that ram pressure stripping may be occurring.

NGC 1961 also shows evidence for ram pressure stripping with an HI extension to the northeast (Shostak et al. 1982). The distorted spiral arms indicate that this galaxy has also had a gravitational encounter; however, no likely companion is apparent. Since, the X-ray observations do not reveal the presence of a dense intragroup medium that could strip the quiescent HI gas we believe that this may be another example where stripping is made more efficient after a gravitational encounter.

We began this study in the hope that selecting galaxies with the extremes of asymmetry and star formation expected for interaction with a surrounding diffuse medium would furnish the best evidence of gas stripping in a relatively simple environment. As it happened, even in these carefully picked instances, evidence for stripping is subtle, and the group environments are rich enough that gravitational interactions with other members still dominate the morphology and star-forming properties of these spirals. The case of NGC 2276 suggests that seeing a combination of these two effects may not be entirely fortuitous – the tidal disturbance may render an H I disk more vulnerable to external hydrodynamical forces than it would otherwise be. The difficulty of separating these effects in nearby galaxies in rather simple environments may serve as a cautionary tale for untangling such effects in clusters and their role in galaxy evolution.

This research made use of the HEASARC, NED, and SkyView databases. We acknowledge support from NASA ROSAT grant NAG5-2703. Some of the VLA data were obtained in collaboration with Jim Condon, who also reduced the radio-continuum data.

REFERENCES

Blair, W.P., Kirshner, R.P., & Winkler, P.F., Jr. 1983, *ApJ* 272, 84

Blair, W.P. & Long, K.S. 1997, *ApJS*, 108, 261

Bushouse, H.A. 1987, *ApJ*, 320, 49

Cayatte, V., Balkowski, C., Van Gorkom, J.M. & Kotanyi, C. 1990, *AJ* 100, 604

Condon, J.J., Frayer, D.T. & Broderick, J.J. 1991 *AJ*, 101, 362

Condon, J.J., Helou, G., Sanders, D.B. & Soifer, B.T. 1990, *ApJS*, 73, 359

Condon, J.J. 1983, *ApJS*, 53, 459

Dahlem, M., Hartner, G.D. & Junkes, N. 1994, *ApJ*, 432, 598

Davis, D.S., Mushotzky, R.F., Mulchaey, J.S., Worrall, D., Birkinshaw, M. & Burstein, D. 1996, *ApJ*, 460, 601

D'Odorico, S. 1978, *Mem Soc Astr Ital* 49, 563

Dopita, M., D'Odorico, S., & Benvenuti, P. 1984, *ApJ*, 236, 628

Fabbiano, G., Kim, D.-W. & Trinchieri G., 1992, *ApJS*, 80, 531

Fabbiano, G., Gioia, I.M. & Trinchieri G., 1988, *ApJ*, 324, 749

Forbes, D. A. & Thomson, R. C. 1992, *MNRAS*, 254, 723

Forman, W., Jones, C. & Tucker W. 1985, *ApJ* 293, 102

Green, P.J., Anderson, S.F. & Ward, M.J. 1992, *MNRAS*, 254, 30

Gruendl, R.A., Vogel, S.N., Davis, D.S., & Mulchaey, J.S. 1993, *ApJL*, 413, L81

Heckman, T.M., Armus, L. & Miley, G.K. 1990, *ApJS*, 74, 833

Howard, S.A., Keel, W.C., Byrd, G.G., & Burkey, J.M. 1993, *ApJ*, 417, 502

Huchtmeier, & Richter, O. G. 1989, *A General Catalog of HI Observations of Galaxies*, (Springer, Berlin)

Hunter, D.A., Gillett, F.C., Gallagher, G.S., III, Rice, W.L. & Low, F.J. 1986, 303, 171

Irwin, J. A. & Sarizan, C. L. 1996, *ApJ* 471, 683

Iskudarian, S.G., 1968, *Astr. Ts.*, 480

Iskudarian, S.G. & Shakhbazian, R.K. 1967, *Astrofizika*, 3, 133

Keel, W.C., 1991, in *Dynamics of Galaxies and Their Molecular Cloud Distributions*, ed. F. Combes and F. Casoli, IAU Sym. 146 (Kluwer), 243

Keel, W.C., Frattare, L.M., & Laurikainen, E. 1993, *BAAS*, 25, 1356

Keel, W.C., Kennicutt, R.C., Jr., van der Hulst, J.M., & Hummel, E. 1985, *AJ*, 90, 708

Kennicutt, R.C., Jr. 1992, *ApJS*, 79, 255

Kennicutt, R.C., Jr., & Garnett, D. R. 1996, *ApJ*, 456, 504

Kennicutt, R.C., Jr., Keel, W.C., van der Hulst, J.M., Hummel, E., & Roettiger, K., 1987, *AJ*, 97, 1022

Kennicutt, R. C., Jr. & Kent, S. M. 1983 *AJ*, 88, 1094

Long, K.S., Blair, W.P., Kirshner, R.P., & Winkler, P.F., Jr., 1990, *ApJS* 61, 73

Longmore, A.J., Hawarden, T.G., Cannon, R.D., Allen, D.A., Mebold, U., Goss, W.M. & Reif, K. 1979, *MNRAS*, 188, 285

Lonsdale, C. J., Helou, G., Good, J. C. & Rice, W. 1985, *Cataloged Galaxies and*

Quasars Observed in the IRAS Survey (Jet Propulsion Laboratory, Pasadena)

Treffers, R. 1993, IAUC 5850

Maia, M. A. G., da Costa, L. N. & Latham, D. W., 1989, ApJS, 69, 809

Malphrus, B.K., Simpson, C.E., Gottesman, S.T., & Hawardem, T.G. 1995, BAAS, 27, 1361

Moore, B., Katz, N., Lake, G., Dressler, A., Oemler, Jr., A. 1996 Nature, 379, 613

Mulchaey, J. S., Davis, D. S., Mushotzky, R. F. & Burstein, D. 1993, ApJ, 404, L9

Mulchaey, J. S., Davis, D. S., Mushotzky, R. F. & Burstein, D. 1996, ApJ, 456, 80

Ponman, T. J. & Bertram, D. 1993, Nature, 363, 51

Thronson H. A. & Telesco C. M. 1986, ApJ, 311, 98

Read, A. M., Ponman, T. J., & Wolstencroft, R. D. 1995, MNRAS, 277, 397

Rubin, V.C., Roberts, M.S., & Ford, W.K., Jr. 1979, ApJ, 230, 35

Romanishin, W. 1983, MNRAS, 204, 909

Sansom, A. E., Dotani, T., Okada, K., Yamashita, A., & Fabbiano, G. 1996, MNRAS, 281, 48

Shakhbazian, R.K. 1968, Astrofizika, 4, 319

Snowden, S. L., McCammon, D., Burrows, D. N. & Mendenhall, J. A. 1994, ApJ, 424, 714

Shostak, G.S., van der Kruit, P.C., Hummel, E., Shaver, P.A., & van der Hulst, J.M. 1982, A&A 115, 293

Stark, A. A., Gammie, C. F., Wilson, R. W., Bally, J., Linke, R. A., Heiles, C. & Hurwitz, M. 1992, Ap. J. Supp., 79, 77

Thronson, H.A., Jr., Telesco, C.M. 1986, ApJ, 311, 98

This 2-column preprint was prepared with the AAS `LATEX` macros v4.0.

Figure Captions

Fig. 1–The HRI data (contours) is overlaying the optical image of NGC 1961 from the digitized sky survey. The X-ray data have been smoothed with a Gaussian with $\sigma=10''$ and the contour levels are (6.66, 7.77, 8.88, 9.98, 11.09, 12.20, 13.31, 14.42, 15.53, 16.64) $\times 10^{-2}$ counts s^{-1} $arcmin^{-2}$.

Fig. 2–The azimuthally averaged X-ray profile of NGC 1961 (triangles) along with the azimuthally average profile of a stellar object from the same image (circles). NGC 1961 has excess emission from $0''.25$ to $\sim 0''.7$.

Fig. 3–The HRI data (contours) is overlaying the optical image of NGC 2276 from the 2-meter telescope at Kitt Peak. The X-ray data have been smoothed with a Gaussian with $\sigma=10''$ and the contour levels are (1.08, 1.21, 1.34, 1.46, 1.59, 1.72, 1.85, 1.98, 2.10, 2.23, 2.36) $\times 10^{-2}$ counts s^{-1} $arcmin^{-2}$.

Fig. 4–The $H\alpha$ image of NGC 2276. North is up and east is to the left. The FOV is $2'$ across.

Fig. 5–The 20 cm radio image of NGC 1961.

Fig. 6–The 20 radio image of NGC 2276. Note the sharp edge of the radio disk to the west of the nucleus.

Fig. 7.–The 21-cm HI line image of NGC 2276. The maps have been smoothed to a resolution of $30'' \times 18''$ (twice the original resolution) with long axis at position angle -10 degrees. Contours are the integrated HI emission with levels at 12, 18, 24, 30, ... 90 mJy/beam. The greyscale represents the velocity field.

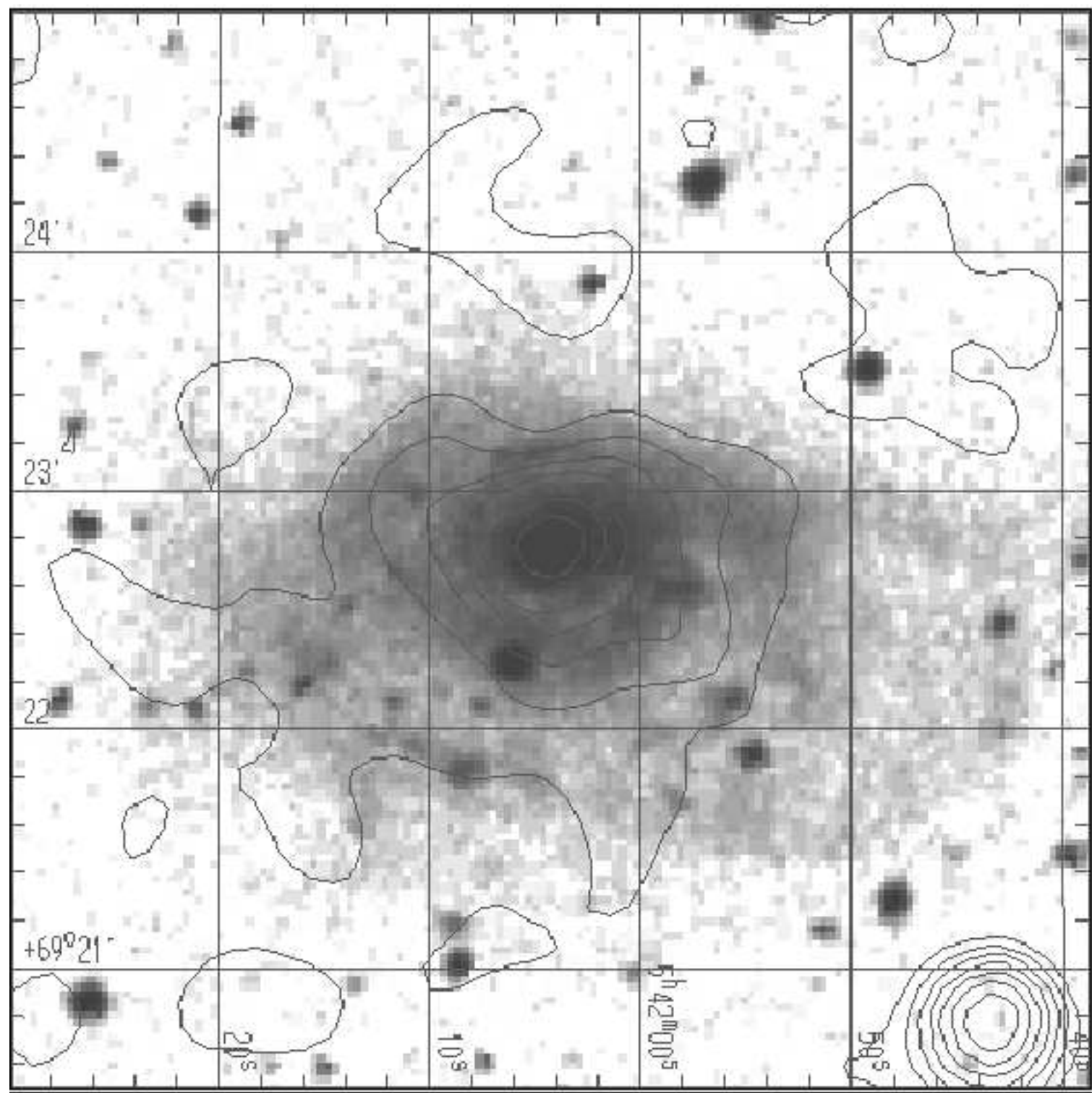


Table 1: *ROSAT* data

Galaxy	Sequence Number	R.A. (J2000)	Dec. (J2000)	Exposure seconds	Observation Date
NGC 1961					
	RP800282	5 ^h 43 ^m 31 ^s	+69° 16'11"	14766	1993 Mar 8-12
	RH600499	5 ^h 42 ^m 4.8 ^s	+69° 22'48"	82704	1994 Mar 11-16
NGC 2276					
	RP800161	7 ^h 26 ^m 53 ^s	+85° 45'00"	5134	1992 Apr 25-27
	RP800512	7 ^h 21 ^m 12 ^s	+85° 42'00"	9034	1993 Aug 22-23
	RP800513	7 ^h 38 ^m 48 ^s	+85° 42'00"	8427	1993 Aug 23
	RH600498	7 ^h 27 ^m 12 ^s	+85° 45'36"	73966	1994 Mar 18-21

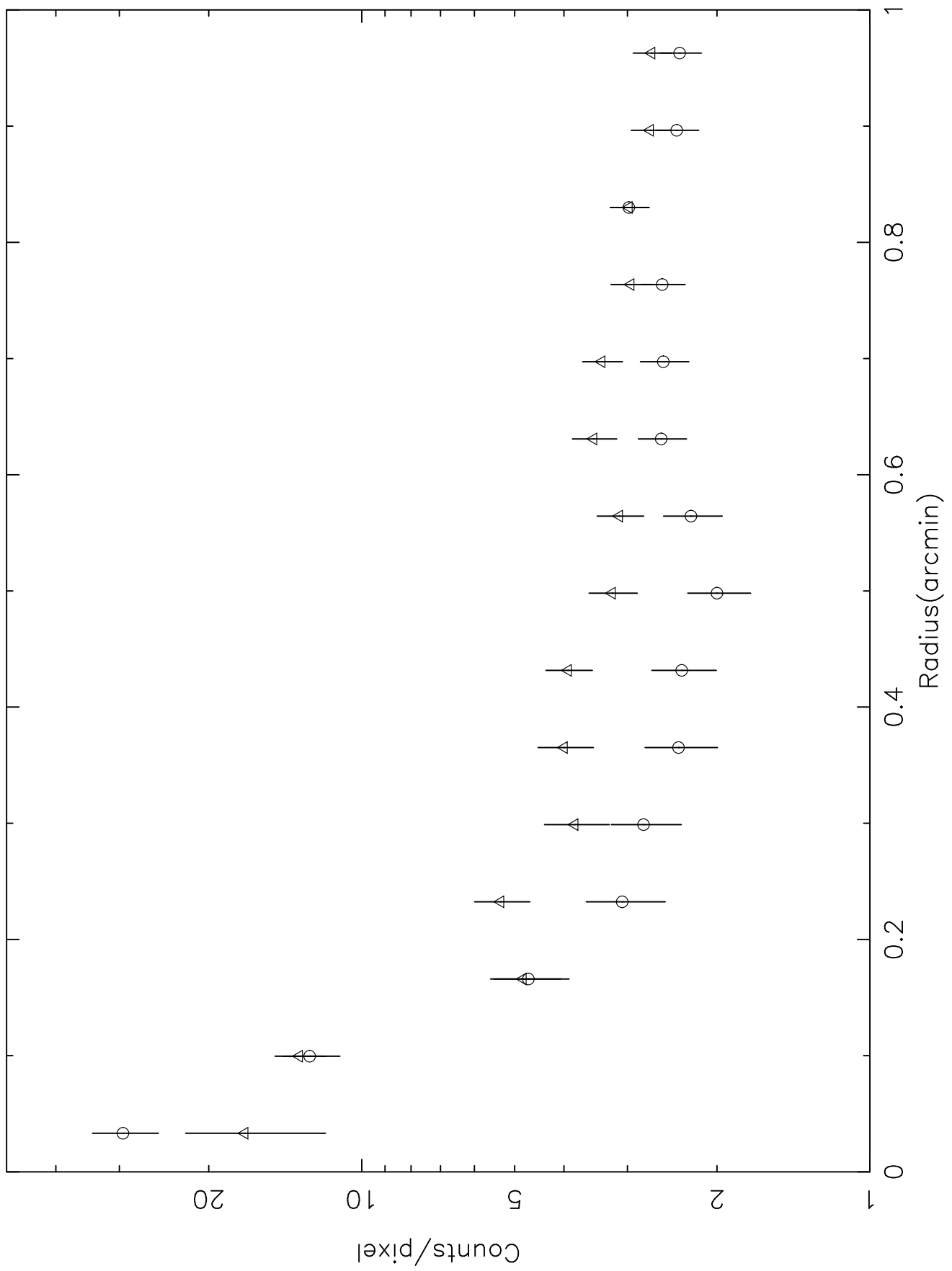


Table 2: Aperture spectrophotometry of H II regions

Region	H α	H β	[O III]	$\lambda 5007$	[S II]	Notes
NGC 2276 - 1	55.5	12.2		19.4	9.9	
NGC 2276 - 2	23.3	5.8		7.0	—	
NGC 1961 nucleus						
NGC 1961 - 20	120	18.4		12.7	15.2	[O II] at 11.7
NGC 1961 - 30-33	81	13.2		12.0	—	[O II] at 27.7

Notes:

Fluxes in units of 10^{-15} erg cm $^{-2}$ s $^{-1}$ Å $^{-1}$ as observed (no reddening correction)

Typical [N II]/H α ratios per galaxy were used to correct to net H α

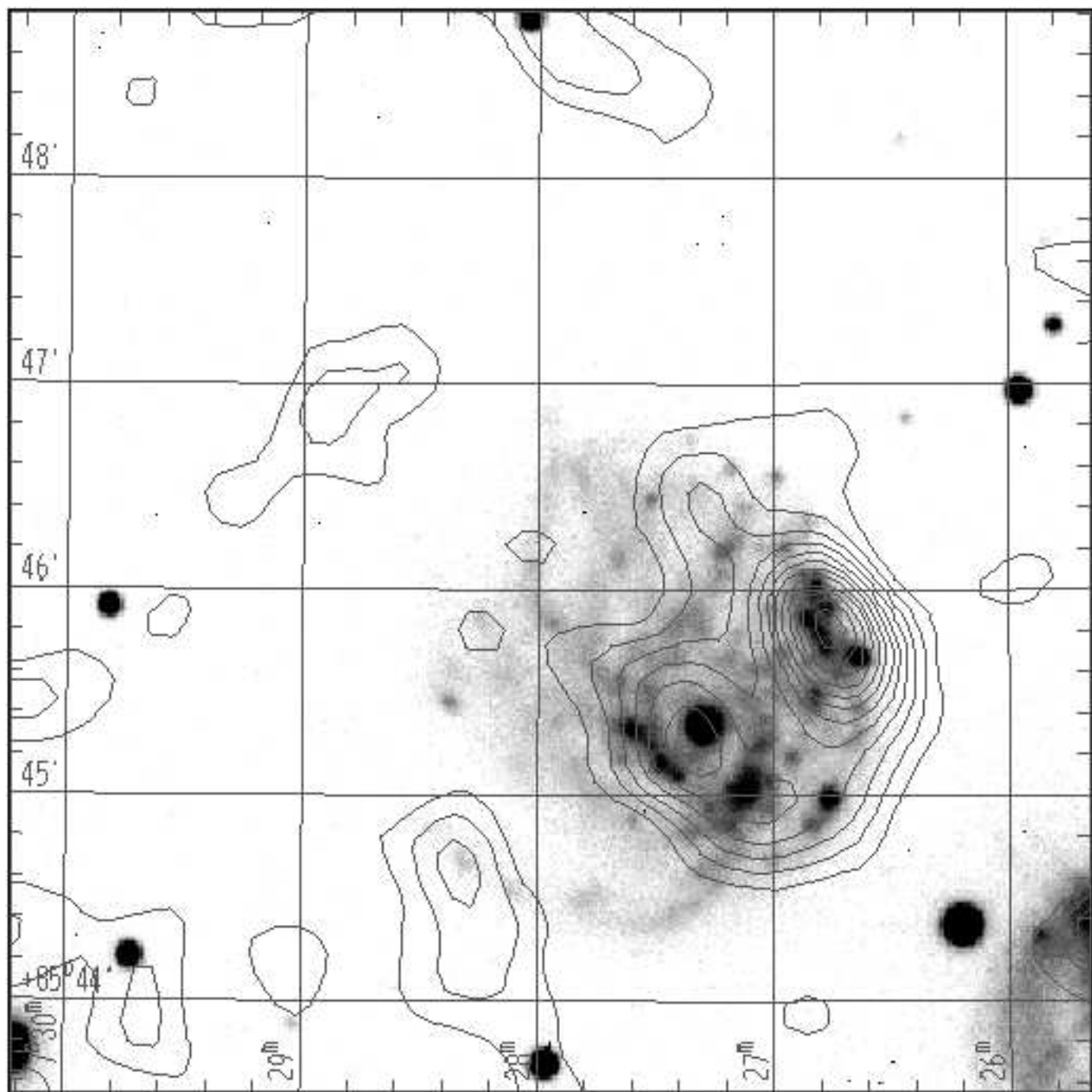


Table 3: H II region measures from narrow-band images

Galaxy	ID	location	F(H α +[N II])	[O III]/H β	H α /H β	[S II]/H α	EW(H α), Å
NGC 2276	nuc	0 0	21.3	0.02	11.5	0.12	56
	1	18N 39W	13.3	1.55	4.7	0.18	120
	2	16S 31W	29.5	1.25	8.4	0.25	232
	3	20N 28W	15.6	0.45	6.5	0.28	312
	4	27N 24W	11.0	0.38	5.1	0.25	160
	5	01S 24W	6.5	<0.03	9.2	0.24	434
	6	08S 10E	14.7	0.16	12.4	0.18	285
	7	00N 18E	8.6	0.08	7.4	0.23	124
	8	26N 55E	4.5	0.89	6.8	0.33	256
	9	01N 35E	4.1	1.06	20.7	0.26	239
	10	38S 03W	4.2	0.63	6.7	0.46	—
	11	11S 05E	7.3	<0.05	9.8	0.28	770:
	12	60N 16W	3.8	1.32	2.4	0.34	147
	13	62N 06W	2.5	0.81	1.9:	0.36	138
	14	16N 19E	2.4	0.16	6.0	0.25	240
	15	22S 26W	10.5	0.55	7.2	0.32	230
	16	06N 37W	5.2	0.77	5.9	0.25	276
	17	13S 17W	6.5	0.14	7.7	0.23	292
NGC 1961	nuc	0 0	5.0				
	1	48W 10N	0.53				
	2	25W 24N	0.27				
	3	17W 19N	0.42				
	4	07W 26N	0.33				
	5	02E 27N	0.94				
	6	11E 26N	0.86				
	7	27E 23N	0.27				
	8	36E 19N	0.86				
	9	36E 15N	1.0				
	10	43E 12N	0.42				
	11	41E 03S	0.95				
	12+13	21E 11S	0.76				
	14	35W 08S	0.89				
	15	36W 04S	0.49				
	16	37W 04N	0.19				
	17	18W 01S	0.29				
	19	72W 24S	0.12				
	20	48W 38S	2.6				
	21	31W 45S	0.07				
	22	26W 48S	0.27				
	23	21W 52S	0.28				
	24+25	21E 55S	2.1				
	26	27E 56S	1.12				
	27	37E 51S	1.4				
	28	46E 48S	1.7				
	29	50E 48S	0.93				
	30	62E 30S	0.94				
	31	62E 34S	0.91				
	32	70E 30S	1.5				

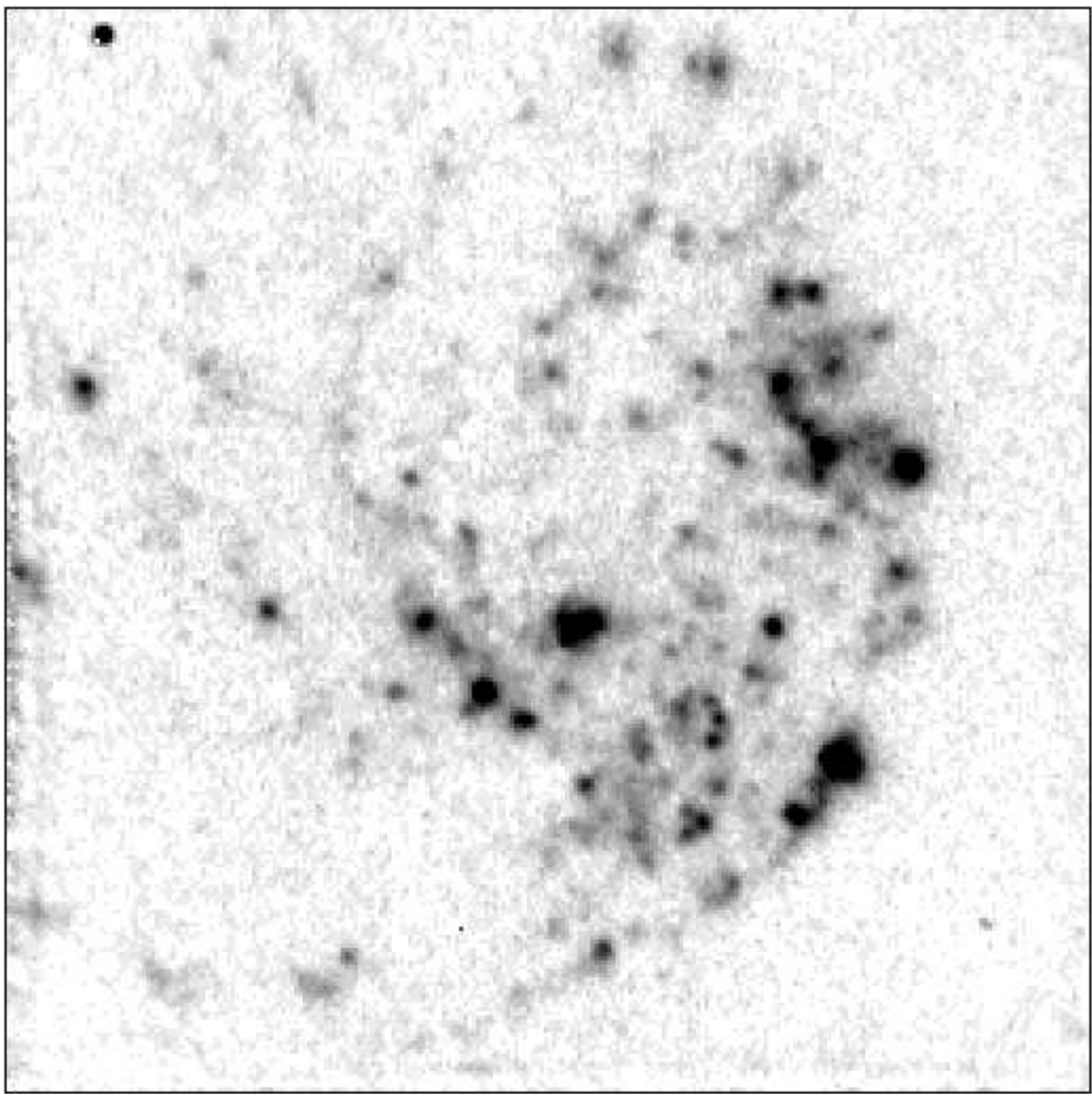
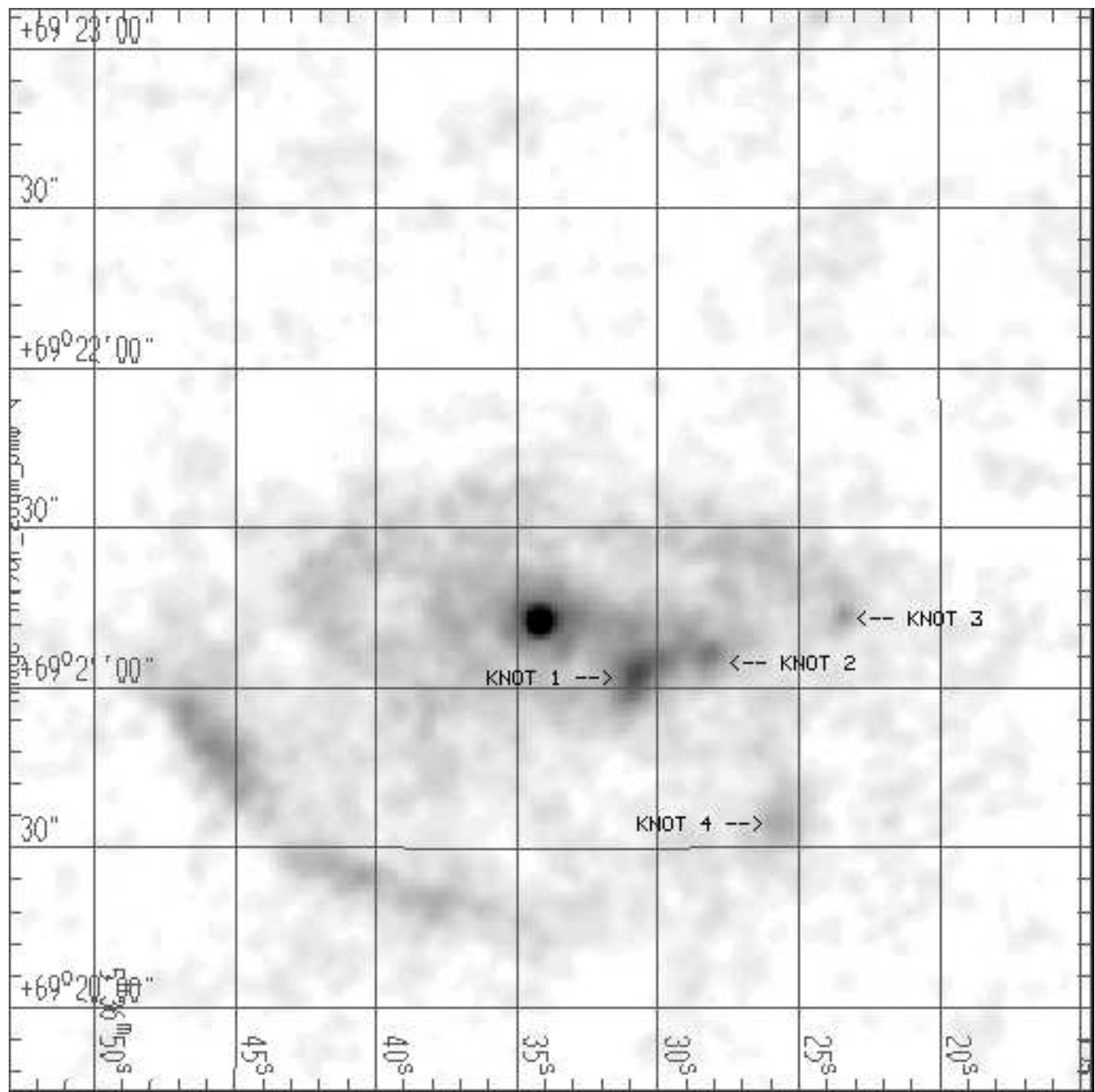
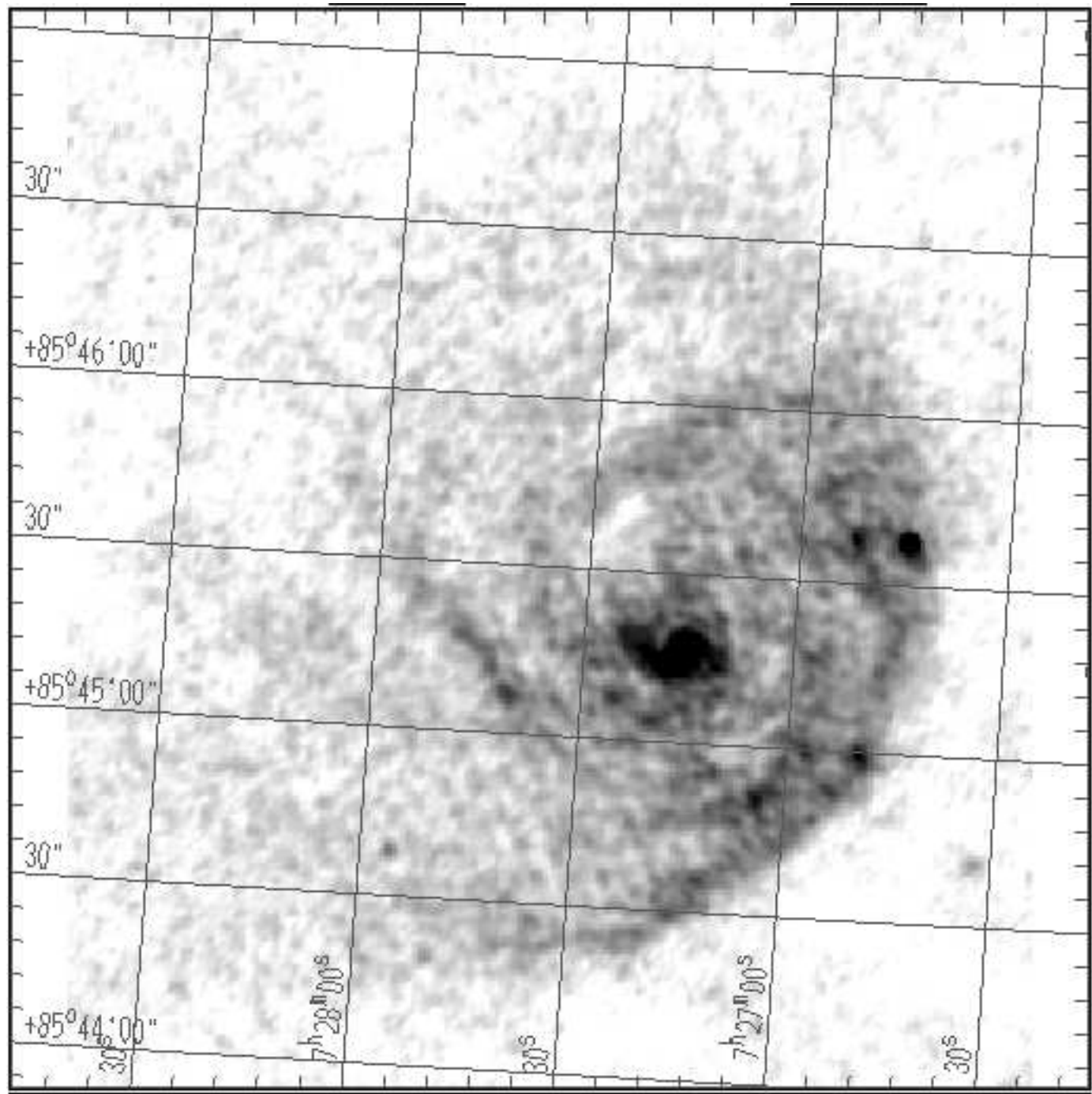


Table 4: Flux & Luminosity data

Galaxy	Band	flux erg s ⁻¹ cm ⁻²	Luminosity erg s ⁻¹
NGC 1961			
	X-ray	1.79×10^{-12}	1.36×10^{41}
NGC 2276			
Total			
	B	2.19×10^{-10}	5.50×10^{43}
	H α	1.35×10^{-12}	3.39×10^{41}
	X-ray	3.33×10^{-12}	1.82×10^{42}
Western Source			
	B	1.84×10^{-11}	4.62×10^{42}
	H α	3.75×10^{-13}	9.41×10^{40}
	X-ray	3.05×10^{-12}	7.66×10^{41}
Southern Source			
	B	1.27×10^{-11}	3.19×10^{42}
	H α	2.10×10^{-13}	5.27×10^{40}
	X-ray	9.78×10^{-13}	2.46×10^{41}
SE Source			
	B	6.81×10^{-11}	1.71×10^{43}
	H α	3.12×10^{-13}	7.83×10^{40}
	X-ray	1.96×10^{-12}	4.92×10^{41}





Plot file version 4 created 23-NOV-1996 12:23:24

GREY: N-2276

IPOL 2276.XMOM1.1

CONT: N-2276

IPOL 2536.2 KM/S

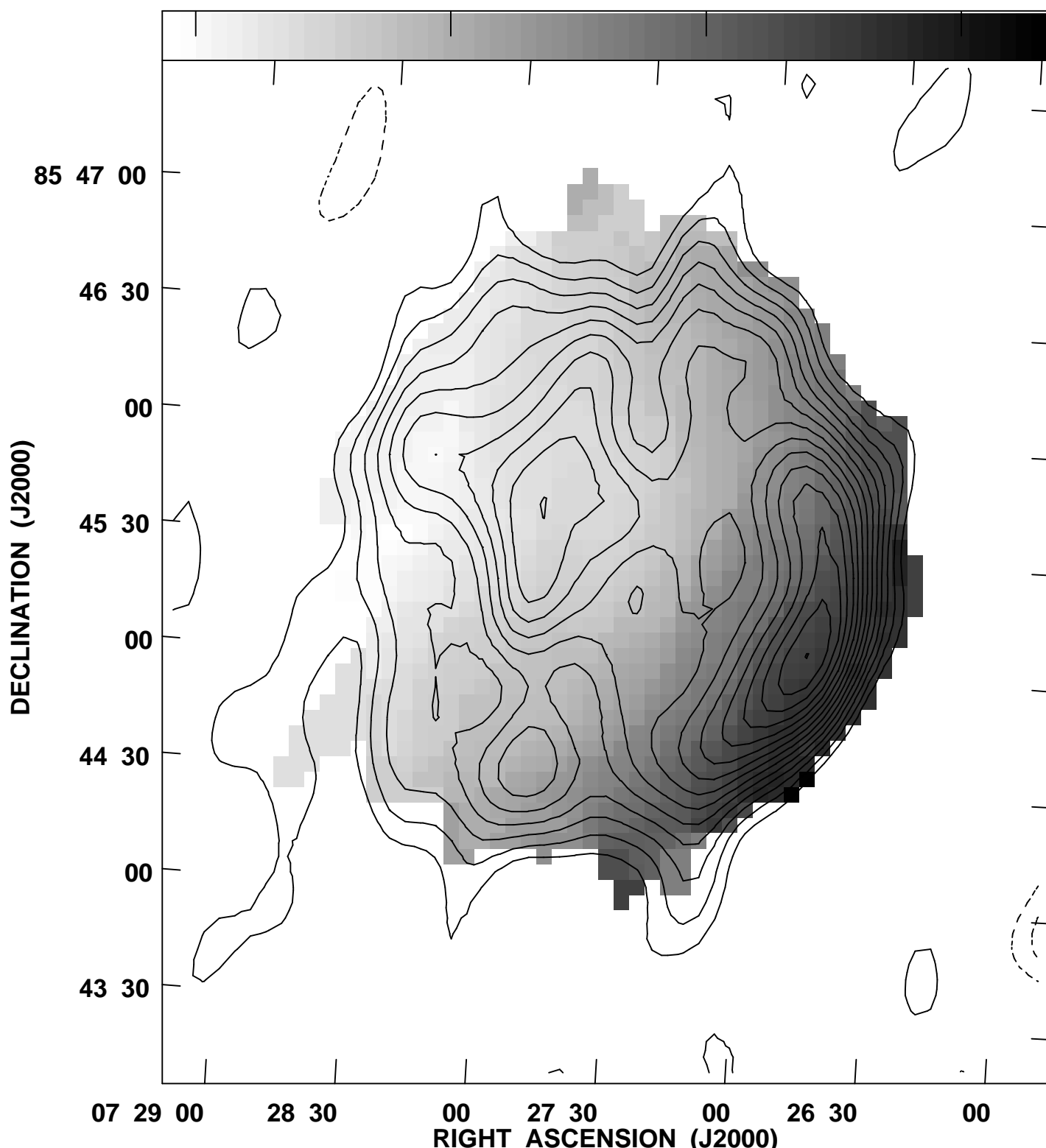
CONVL19-39.SQASH.1

2350

2400

2450

2500



Grey scale flux range= 2345.6 2515.2 Kilo METR/SEC

Peak contour flux = 9.0528E-02 JY/BEAM

Levs = 6.0200E-03 * (-5.00, -4.00, -3.00,
-2.00, 2.000, 3.000, 4.000, 5.000, 6.000,
7.000, 8.000, 9.000, 10.00, 11.00, 12.00,
13.00, 14.00, 15.00, 16.00)